



Published in final edited form as:

Proc IEEE Int Conf Comput Vis. 2007 ; : 1–8.

## Diffusion Tensor Estimation by Maximizing Rician Likelihood

Bennett Landman, Pierre-Louis Bazin, and Jerry Prince

Johns Hopkins University School of Medicine Baltimore, MD 21205

Bennett Landman: blandma1@jhmi.edu; Pierre-Louis Bazin: pbazin1@jhmi.edu; Jerry Prince: prince@jhu.edu

### Abstract

Diffusion tensor imaging (DTI) is widely used to characterize white matter in health and disease. Previous approaches to the estimation of diffusion tensors have either been statistically suboptimal or have used Gaussian approximations of the underlying noise structure, which is Rician in reality. This can cause quantities derived from these tensors — e.g., fractional anisotropy and apparent diffusion coefficient — to diverge from their true values, potentially leading to artifactual changes that confound clinically significant ones. This paper presents a novel maximum likelihood approach to tensor estimation, denoted Diffusion Tensor Estimation by Maximizing Rician Likelihood (DTEMRL). In contrast to previous approaches, DTEMRL considers the joint distribution of all observed data in the context of an augmented tensor model to account for variable levels of Rician noise. To improve numeric stability and prevent non-physical solutions, DTEMRL incorporates a robust characterization of positive definite tensors and a new estimator of underlying noise variance. In simulated and clinical data, mean squared error metrics show consistent and significant improvements from low clinical SNR to high SNR. DTEMRL may be readily supplemented with spatial regularization or a priori tensor distributions for Bayesian tensor estimation.

### 1. Introduction

Diffusion tensor imaging (DTI) provides unique insights into *in vivo* tissue structure through contrasts sensitive to the directional diffusion of water within restricted environments [2]. Derived tensor contrasts, including fractional anisotropy (FA) and mean diffusivity (MD), have been widely applied to characterize cytoarchitectural changes related to damage in cerebral white matter (e.g. see a review by Horsfield and Jones [11]). At low signal to noise ratios (SNRs), estimated contrasts tend to systematically diverge from their true values (increased bias in addition to increased variability), which leads to artifactual changes that confound clinically significant ones [3]. This study presents a maximum likelihood (ML) approach of estimating tensors from DTI data that accounts for (1) non-Gaussian distributed noise and (2) statistical dependence between observations to minimize bias. This novel approach specifically addresses the joint likelihood of all observations given a tensor model (as opposed to the marginal likelihood of each observation), denoted Diffusion Tensor Estimation by Maximizing Rician Likelihood (DTEMRL).

In DTI studies, the degree and orientation of random thermal (Brownian) motion of water are inferred from the signal intensity obtained during sensitized, “diffusion weighted” (DW) acquisitions relative to a reference. A typical DTI study consists of a reference image and series of 6 or more DW images, each of which are attenuated according to the diffusivity along a particular linear direction. The absolute intensity depends on the local relaxation properties (e.g., T1, T2, PD) of the tissue which are not directly linked to diffusivity. The ratio between the DW and reference signals provides the relevant information. The 3D diffusivity is modeled as a tensor fit to these ratios.

Current methods of computing tensors do not fully account for the physical noise structure in magnetic resonance (MR) data. The noise on acquired images is well characterized by independent Rician distributions [10]. Independence between the noise on the intensities at the same location in different images is lost when the ratio between DW and reference images is computed because a common denominator is used. The most prevalent tensor estimation method, the log-linear minimum mean squared error (LLMMSE) approach [2], assumes the noise to be independently and identically Gaussian distributed on the logarithms of the ratios. In support of the LLMMSE approach, Gudbjartsson *et al.* [10] demonstrated that the distribution of the logarithm of ratio of Rician random variables is “nearly Gaussian” for SNRs greater than 2:1.

Methods for compensating for Rician bias in DTI have been proposed primarily in two categories, (1) characterization of the noise structure in single images and (2) spatial regularization of DTI data. Sijbers *et al.* [19] presented an ML approach for Rician bias compensation of single MR images. Koay *et al.* [13] demonstrated an exact solution and extended the method for images from multiple coils. Jones *et al.* [12] presented an estimation method that incorporates noise level estimation. Salvador *et al.* [18] reviews distribution assumptions and describes a weighted least squares procedure for addressing non-Gaussianity. Recent abstracts indicate that a Rician noise model is more accurate than Gaussian estimation (e.g., [1]). Spatial filtering of DTI data to compensate for Rician noise has been proposed in multiple contexts, including with wavelets [15], variational methods [22], anisotropic smoothing [8], and edge preserving partial differential equations [6].

In this work, spatial regularization is avoided to demonstrate improvements possible without compromise to spatial accuracy. The DTEMRL framework can readily incorporate spatial consistency constraints as in the Frandsen *et al.* Bayesian tensor field regularization [9] or the Basu *et al.* maximum *a posteriori* smoothness integrating Rician bias compensation [4]. In contrast to these approaches, DTEMRL assesses the likelihood as the joint probability of observations rather than as a spatial regularization problem given Rician marginal likelihoods.

In the tensor model of diffusion, the probabilistic motion of water is independent along three orthogonal axes (i.e., tensor eigenvectors) with three independent diffusivities (i.e., tensor eigenvalues). Since physical diffusivities cannot be negative, tensors that arise from diffusion must be positive definite. However, common tensor estimation methods, including LLMMSE, may result in tensors with negative eigenvalues. Nonlinear approaches to limit solutions to the manifold of positive definite tensors have been proposed by Tschumperlé *et al.* [21], Niethammer [14], and Cox *et al.* [7]. These methods have not specifically addressed both the eigenvalue constraints and the Rician noise distributions.

Despite the “near-Gaussian” distributions of DTI experimental data, DTEMRL offers substantial improvements at high SNRs, up to and including 40:1. In simulations, mean squared error metrics demonstrate consistent and significant improvements with low clinical to high SNR acquisitions.

## 2. Theory

### 2.1. Diffusion Tensor Imaging

The DW images that form the basis of DTI are typically created by augmenting a conventional spin echo MR study with sensitization magnetic field gradients. Relative to a traditional spin-echo reference, these “diffusion weighting gradients” produce intensity changes that are dependent on the orientation of the magnetic field gradients relative to the

underlying tissue microstructure. The tensor model of diffusion models observed intensities by the Stejskal-Tanner expression [2],

$$S_i = S_0 e^{-b g_i^T D g_i} \quad (1)$$

where  $S_i$  is the observed signal for the  $i$ th direction,  $S_0$  is the reference signal,  $b$  is a signal attenuation constant (the “b-value”),  $g_i$  is the unit direction vector of  $i$ th DW direction, and  $D$  is the diffusion tensor, a symmetric  $3 \times 3$  matrix,

$$D = \begin{bmatrix} D_{xx} & D_{xy} & D_{xz} \\ D_{xy} & D_{yy} & D_{yz} \\ D_{xz} & D_{yz} & D_{zz} \end{bmatrix}. \quad (2)$$

The DW directions and b-value are determined by experimental settings and are generally known before data acquisition. When a set of six or more non-collinear (and not mutually coplanar) DW directions are acquired, the tensor may be linearly estimated from the logarithm of ratios [2]:

$$\begin{bmatrix} \ln \left( \frac{S_1}{S_0} \right) \\ \vdots \\ \ln \left( \frac{S_N}{S_0} \right) \end{bmatrix} = \begin{bmatrix} (g_x^2 & 2g_x g_y & 2g_x g_z & g_y^2 & 2g_y g_z & g_z^2)_1 \\ \vdots & \vdots & \vdots & \vdots & \vdots & \vdots \\ (g_x^2 & 2g_x g_y & 2g_x g_z & g_y^2 & 2g_y g_z & g_z^2)_N \end{bmatrix} \begin{bmatrix} D_{xx} \\ D_{xy} \\ D_{xz} \\ D_{yy} \\ D_{yz} \\ D_{zz} \end{bmatrix}. \quad (3)$$

Linear regression of the right hand side “G” matrix on the left hand side “log-observations ratio” vector is an ML estimate of the diffusion tensor when the noise on  $\ln S_i/S_0$  is independently and identically Gaussian distributed. The ratio between DW and reference intensity is known as the apparent diffusion coefficient (ADC).

## 2.2. Noise in MR Imaging

The physical MR observations of complex-valued Fourier coefficient images are well described by Gaussian distributions. In DTI however, the reference and DW images are real-valued magnitude images. Thus, the noise on individual MR observations follows a Rician distribution,

$$p(x; \nu, \sigma) = \frac{x}{\sigma^2} e^{-\frac{x^2 + \nu^2}{2\sigma^2}} I_0 \left( \frac{x\nu}{\sigma^2} \right), \quad (4)$$

where  $x$  is the observed signal,  $\nu$  is the true mean intensity,  $\sigma$  is the standard deviation of noise on the original complex valued image, and  $I_0$  is a zeroth order modified Bessel function of the first kind. We define SNR as the magnitude of the noise-free signal divided by the standard deviation of the noise on the original complex image ( $\sigma$ ). The distribution of the ratio of Ricians may be solved for special cases or evaluated numerically, but a convenient closed form expression is not known. At low SNR, this distribution exhibits significant non-Gaussian skew. Furthermore, a single common reference image is used for all DW images to compute ADCs, so the ADCs are not independent observations. Finally, the LLMMSE model makes no constraints on the eigenvalues of the resulting tensor, while

physical diffusivities (the quantity associated with the tensor eigenvalues) cannot be negative.

### 2.3. Maximum Likelihood Estimation

Consider a DTI study with a reference image and  $NDW$  images. Since the noise on each acquired image is independent, the log-likelihood,  $L$ , of the observed data can be computed by combining Eq. 1 and Eq. 4:

$$L(\widehat{D}, \widehat{S}_0, \widehat{\sigma}_{0:N}; S_{0:N}) = \sum_{i=0}^N \ln p(S_i; \widehat{S}_0 e^{-bg_i^T \widehat{D}_{S_i}}, \widehat{\sigma}_i) \quad (5)$$

where  $\widehat{D}$  is the tensor estimate,  $\widehat{S}_0$  is the reference signal estimate, and  $\widehat{\sigma}_i$  is the estimated noise level on image  $i$ . For notational convenience,  $g_0$  is defined as the zero vector.

Both the reference signal intensity and noise level are anatomically dependent, spatially varying, and, in general, unknown. The noise level is independent of DW, so a single  $\sigma$  parameter per location is sufficient. If different numbers of averages are used for different images, then the  $\sigma_i$  parameter may be computed from the single baseline parameter by a constant scalar. So, the ML approach requires estimating eight parameters as opposed to a traditional LLMMSE method which only estimates the six tensor parameters.

### 2.4. Model Parameterization

The globally optimal ML solution does not depend on the diffusion tensor parameterization, yet investigation reveals differing susceptibilities to local maxima and sensitivity to numeric precision (not shown). Diffusion tensors are commonly represented by the six unique matrix coefficients (Eq. 2). In DTEMRL, diffusion tensor are represented by three degree of freedom rotation ( $R$ ) and eigenvalue ( $\Lambda$ ) matrices:

$$D = R^T \Lambda R. \quad (6)$$

This representation readily enables constraints on the eigenvalues. In particular, the diffusion tensor is restricted to the space of positive definite tensors by parameterizing each eigenvalue by its logarithm:

$$\Lambda = \begin{vmatrix} e^{l_1} & & \\ & e^{l_2} & \\ & & e^{l_3} \end{vmatrix}, \quad (7)$$

where  $l_j$  is the  $j$ th eigenvalue parameter and  $e^{l_j}$  is the  $j$ th eigenvalue. The classical representation of rotation matrices uses Euler angles. Yet, Euler angles are numerically difficult to jointly optimize because they are inhomogeneous, correlated, and have numerous singularities. DTEMRL exploits an alternative representation based on Rodrigues' analysis and related to the quaternion form [5]:

$$R = \begin{vmatrix} 1-2b^2-2c^2 & 2ab-2c\gamma & 2ac+2b\gamma \\ 2ab+2c\gamma & 1-2a^2-2c^2 & 2bc-2a\gamma \\ 2ac-2b\gamma & 2bc+2a\gamma & 1-2a^2-2b^2 \end{vmatrix}, \quad (8)$$

where  $a$ ,  $b$ , and  $c$  are the angular parameters,  $\gamma = \sqrt{1-a^2-b^2-c^2}$ , and  $a^2 + b^2 + c^2$  is restricted to  $[0, 1]$ . The derivatives of the parameters are equal for all parameters, and there is a single singularity at  $\gamma = 0$ . The remaining two parameters,  $S_0$  and  $\sigma$ , in DTEMRL are represented

in their native forms for efficiency because non-negativity problems were not encountered in practice.

### 3. Methods

#### 3.1. Model Initialization

The numeric maximization of likelihood (Eq. 5) requires an initial parameter estimate to seed the optimization. The initial tensor parameters ( $\hat{l}_{10}, \hat{l}_{20}, \hat{l}_{30}, \hat{a}_0, \hat{b}_0, \hat{c}_0$ ) were derived from an LLMMSE tensor estimate. Negative eigenvalues and small magnitude eigenvalues (less than  $1 \times 10^{-6}$ ) from the LLMMSE result were replaced with  $1 \times 10^{-6}$ . The estimated reference signal  $\hat{S}_{00}$  was initialized to the observed reference signal  $S_0$ .

Initial estimation of the noise level  $\hat{\sigma}_0$  in DTI is more involved. It has often been proposed to estimate the noise level from background data [19]. Yet, clinical image reconstruction programs employ background suppression and signal equalization, especially with parallel imaging reconstruction (e.g. SENSE [17]). Therefore, the noise level in the background is not representative of the noise level within tissue. Furthermore, noise level varies with coil sensitivity, which may be readily visualized on clinical data [12]. In DTI, images are typically up-sampled by zero-padding complex-valued Fourier coefficient images, so the local noise structure is highly correlated. Hence, estimation of noise level from local, homogeneous regions is difficult.

The physical noise level ( $\sigma$ ) at any given voxel is not dependent on diffusion weighting. However, the number of averages used in the observed data must be taken into account. An additional complicating factor is that signal intensity varies on the reference ( $S_0$ ) and each of the individual DW images ( $S_j$ ). To overcome this difficulty, an estimate of noise level ( $\tilde{\sigma}$ ) is formed based on a repeated acquisition (i.e., a complete duplicate set of reference and DW images), which is commonly available in practice. For voxels with high signal intensity, the intensity distribution is approximately Gaussian but with variable mean. The differences between repeated observations with the same diffusion weighting are also approximately Gaussian, but with zero mean and  $\sqrt{2}$  increased standard deviation. Since the distribution of the difference of Gaussian random variables does not depend on the original mean, differences from the reference and DW images may be treated as repeated observations from the same distribution. Accordingly, we form the following estimator of  $\tilde{\sigma}$  based on the sample standard deviation while correcting for the  $\sqrt{2}$  increase in standard deviation,

$$\tilde{\sigma} = \sqrt{\frac{1}{2N} \sum_{i=0}^N (\xi_i d_i - \frac{1}{N+1} \sum_{i=0}^N \xi_i d_i)^2}, \quad (9)$$

where  $d_i$  is the difference in signal intensities between the  $i$ th repeated pair of images (with the same diffusion weighting) and  $\xi_i$  is the square root of the number of (k-space) averages acquired for the  $i$ th image.

Estimates of  $\tilde{\sigma}$  using Eq. 9 tend to exhibit low SNR and spatial variations that are inconsistent with coil sensitivity profiles. Therefore, we regularize the initial noise field  $\tilde{\sigma}$  using Chebyshev polynomial regression on non-background voxels with a third degree two-dimensional polynomial to create physically realistic noise level estimates ( $\hat{\sigma}$ ). Although other regularizers are possible, we note that Chebyshev polynomials are numerically stable and have been previously used to model coil sensitivity profiles [16].

### 3.2. Maximum Likelihood Estimation

ML estimates of tensor parameters were obtained by numeric optimization of Eq. 5 using the Nelder-Mead simplex algorithm in Matlab (Mathworks, Natick, MA). To improve stability, optimization proceeded in three stages. First, a refined estimate of the tensor parameters was determined by fixing the noise and baseline intensity estimates,

$$\{\widehat{l}_{11}, \widehat{l}_{21}, \widehat{l}_{31}, \widehat{a}_1, \widehat{b}_1, \widehat{c}_1\} = \operatorname{argmax}_{l_1, l_2, l_3, a, b, c} L(\bullet; \widehat{S}_{00}, \widehat{\sigma}_0). \quad (10)$$

Second, the estimates of reference intensity and noise level were refined holding the tensor definition constant,

$$\{\widehat{S}_0, \widehat{\sigma}\} = \operatorname{argmax}_{S_0, \sigma} L(\bullet; \widehat{l}_{11}, \widehat{l}_{21}, \widehat{l}_{31}, \widehat{a}_1, \widehat{b}_1, \widehat{c}_1). \quad (11)$$

Third, the tensor parameters were refined based on the updated estimated reference intensity and noise level,

$$\{\widehat{l}_1, \widehat{l}_2, \widehat{l}_3, \widehat{a}, \widehat{b}, \widehat{c}\} = \operatorname{argmax}_{l_1, l_2, l_3, a, b, c} L(\bullet; \widehat{S}_0, \widehat{\sigma}). \quad (12)$$

In practice, iterative optimization is possible to avoid local minima. However, empirical simulations found that a single pass was within 0.02 percent of the maximum likelihood found after 10 iterations under realistic clinical conditions.

### 3.3. Simulation Study

Simulation experiments were performed with prolate tensors (i.e., tensors with identical second and third eigenvalues). The maximum (parallel) diffusivity was set to  $2 \times 10^{-3} \text{ mm}^2/\text{s}$  and the radial diffusivities were adjusted to create tensors with fractional anisotropies of 0, 0.2, 0.5, and 0.8. Simulated DTI studies were conducted at b-value of  $1000 \text{ s/mm}^2$  with the 30 DW directions described by Jones and tabulated by Skare *et al.* [20]. One thousand Monte Carlo iterations were performed at each of 36 linearly spaced noise levels between 5:1 and 40:1. First, the reliability of LLMMSE and DTEMRL tensor estimation methods were assessed when noise estimates were correctly initialized ( $\widehat{\sigma} = \sigma$ ). Second, the simulations were repeated with the initial noise level randomly set to either 80 percent or 120 percent of the correct value ( $\widehat{\sigma} = \sigma \pm 0.2\sigma$ ). Note that DTEMRL adapts its estimate of noise level based on observed data (Eq. 11) both when the noise level was correctly and incorrectly specified. Both methods were evaluated in terms of the mean squared errors (MSEs) on the tensor coefficients and derived scalar measures.

### 3.4. Empirical Study

Repeated acquisitions of a single subject were acquired from the Biomedical Informatics Research Network (BIRN) repository (<http://www.nbirn.net>). Briefly, the dataset consists of 15 DTI scans of a healthy 24 year old male volunteer, acquired using a 1.5T MR unit (Intera, Philips Medical Systems, Best, The Netherlands) with body coil excitation and a six channel phased array SENSE head-coil for reception. Each DTI dataset was acquired with the following imaging protocol. A multi-slice, single-shot EPI (SENSE factor = 2.0), spin echo sequence ( $90^\circ$  flip angle, TR/TE = 3632/100 ms) was used to acquire 25 transverse slices parallel to the line connecting the anterior and posterior commissures, with no slice gap and 2.5 mm nominal isotropic resolution (FOV =  $240 \times 240$ , data matrix =  $96 \times 96$ ,

reconstructed to  $256 \times 256$ ). A slice at the level of the corpus callosum was selected for comparative processing. Diffusion weighting was applied along 30 DW directions described by Jones *et al.* [20] with a b-value of  $1000 \text{ s/mm}^2$ . Five minimally weighted reference images ( $S_0$ ) were acquired and averaged on the scanner as part of each DTI dataset. The SNR on the resulting  $S_0$  images was approximately 23:1 within the corpus callosum (white matter). The total scan time to acquire one DTI dataset was 2 min 18s. DTI data were corrected for subject motion with a public DTI software package.

Empirical noise level was estimated by computing the standard deviation on each voxel measurement type (15 observations per voxel per image), averaging across all images (1 reference and 30 DW images), and fitting a Chebyshev model. The pairwise noise estimation procedure was evaluated on all 105 combinations (15 choose 2) of two data sets to evaluate its reliability.

LLMMSE and DTEMRL methods were run on each of the 15 datasets. As the noise level initialization procedure requires two datasets, an arbitrary second dataset was used in the noise field initialization stage. To provide a “high SNR” comparison, both methods were also run on all acquired data (15 reference images and 450 DW images).

## 4. Results

### 4.1. Simulation

Simulations with correctly initialized noise level ( $\hat{\sigma}_0 = \sigma$ ) demonstrate that DTEMRL exhibits two distinct modes of behavior depending on the relationship between SNR and FA (Fig. 1 A, B, D, E). When SNR is above a threshold, then DTEMRL results in substantial improvement in the estimation of tensor coefficients. The simulated methodological differences with SNR greater than 20:1 demonstrate a mean improvement in tensor coefficient MSE of  $4.4 \pm 1.7\%$ ,  $6.9 \pm 1.1\%$ ,  $20.3 \pm 1.3\%$ , and  $33.3 \pm 1.68\%$  (mean  $\pm$  standard deviation) for tensor FAs of 0, 0.2, 0.5, and 0.8, respectively (Fig. 1 B). At SNRs less than 18:1, 13:1, 10:1, and 6:1 for tensor FAs of 0, 0.2, 0.5, and 0.8 respectively, DTEMRL reliability is less than that of LLMMSE.

Initialization with an incorrect noise level degrades DTEMRL performance, which corresponds to approximately a 5:1 decrease in SNR. Yet, we observe the same bimodal behavior as with correctly initialized simulations. Above an SNR of 25:1, there are mean changes in tensor coefficient MSE of  $-2.1 \pm 3.1\%$ ,  $4.4 \pm 0.92\%$ ,  $19.8 \pm 1.2\%$ , and  $33.1 \pm 1.5\%$  (mean  $\pm$  standard error) for tensor FAs of 0, 0.2, 0.5, and 0.8, respectively (Fig. 1 C). Misspecification decrease performance in isotropic areas, yet differences after compensating for the SNR shift are not significant for FA 0.2 ( $p=0.08$ , 0.78, 0.94 for FA=0.2, 0.5, 0.8). For isotropic tensors, reliability is significantly degraded ( $p < 0.05$ ).

### 4.2. Noise Level Estimation

The empirically estimated (“high SNR”) noise level (Fig. 2 A) demonstrates strong spatial variability, with the noise level near the center of brain more than double that in the cortex. The spatial variability and general structure of the noise field are preserved with Chebyshev polynomial regularization (Fig. 2 B). The bias between the high SNR regularized noise level (Fig. 2 B) and the estimated regularized field from pairs of DW datasets is less than 5 percent bias (Fig. 2 C), which indicates a high degree of accuracy even when using limited data. The reliability of estimates from pairs of DW datasets is very high; variability across the brain was much less than 5 percent (Fig. 2 D), except near the frontal poles which are highly susceptible to distortion artifact.

### 4.3. Tensor Estimation with Acquired Data

The LLMMSE and DTEMRL methods demonstrate consistent differences even when using all available clinical data. FA was higher in white matter structures (Fig. 3 A, B) with the degree of difference proportional to tissue anisotropy. On single datasets, LLMMSE resulted in higher FA in gray matter (note putamen and globus pallidus) and lower FA in white matter (Fig. 3 C, D). Variability of the LLMMSE was greater across the brain except for the ventricles (Fig. 3 E, F).

To assess systematic differences in estimated FA with LLMMSE and DTEMRL, voxels were binned by the FA estimated with DTEMRL. For voxels in each bin, the mean methodological differences in FA was computed. These mean differences are indicative of the known systematic bias with LLMMSE and depend on FA (Fig 4). At low FA, the bias is slightly positive, with DTEMRL resulting in slightly lower FA. At increasing FA, the bias shifts negative with DTEMRL resulting in higher FA.

The DTEMRL variability of tensor coefficients was reduced by more than 40 percent in white matter, unchanged in gray matter, and increased in the cerebrospinal fluid (Fig. 5 A). The DTEMRL variability of MD was slightly reduced in white matter and substantially increased in the cerebral spinal fluid (Fig. 5 B).

The “shape” of a diffusion tensor (i.e., orientation and eigenvalues) may be visualized by rendering the directional ADC functions. The visual variability of ADC functions estimated from distinct datasets provide a qualitative sense as to degree of improvements with DTEMRL over LLMMSE (Fig. 6). The illustrations show representative white matter regions of interest. DTEMRL results in more reliable orientation estimates (a narrow angular spread of the major axis of the “peanuts”) and eigenvalues (consistent size of the “peanut” along each axes).

## 5. Discussion

### 5.1. Tensor Estimation

Simulations demonstrate that tensor estimates may be considerably improved by exploiting the Rician noise distributions of MR data (Fig. 1). However, using this information requires estimating two additional parameters (the intensity of the reference signal and noise level) which are not needed for LLMMSE. Thus, a minimum of seven diffusion weighted images and a reference image are required. At moderate and high SNR, DTEMRL improves the reliability of tensor estimation, and the magnitude of improvements is greater for tensors of high anisotropy. For very low SNR, simulations indicate that the DTEMRL method may reduce estimation performance, likely due to variability introduced with the additional parameters. These results suggest the need for regularization of DTEMRL when the SNR is very low or, similarly, when very few DW images are acquired. Experiments with clinical data demonstrate consistent improvements with DTEMRL. DTEMRL operates in the stable, “high SNR” regime for DTI studies using only one acquisition at 1.5T. Typically, 3 to 5 averages are acquired at 1.5T to improve SNR by 70 to 120 percent. Simulations indicate that improvement in SNR would reduce the likelihood that DTEMRL would continue to outperform LLMMSE without decreasing proportional improvement of DTEMRL over LLMMSE.

Experiments with clinical data demonstrate that DTEMRL remains robust in spite of the approximate nature of the tensor model, presence of artifact, and spatially heterogeneous tissue. Reproducibilities of FA (Fig. 3 E, F), tensor coefficients (Fig. 5 A), and MD (Fig. 5 B) are greater (lower standard deviation) for DTEMRL than LLMMSE. The percent improvements are greatest for tensor coefficients in white matter. Negative impacts of

reduced SNR are mitigated by high FA. Once data is of sufficient SNR for DTEMRL to offer improved reliability, the proportional benefits are essentially constant across SNR while the magnitude of the improvement increases with FA (Fig. 1 B, E). Although numeric optimization depends upon the initialization accuracy, DTEMRL tensor estimates remain stable in spite of a 20 percent mis-specification of initial noise level (Fig. 1 C, F).

Without a valid ground truth, the full reliability cannot be assessed with *in vivo* data. The “high SNR” estimates are not a suitable proxy because the estimates with LLMMSE and DTEMRL are different. In LLMMSE, including additional observations reduces the variability in the DW image intensity, but also reinforces bias on each DW image. With DTEMRL, additional observations enable refinement of the noise estimate, and reduce both variability and bias in the estimated DW image intensities during tensor estimation. Low SNR tends to positively bias FA in regions of low anisotropy and negatively bias FA in regions of high anisotropy with the LLMMSE method [12]. The systematic bias between FA estimated with LLMMSE and DTEMRL (Fig. 4) is in the opposite direction, which suggests that DTEMRL would reduce bias in the estimated tensors. However, additional acquisitions using k-space averaging and/or complex-valued imaging data are required to generate unbiased, high SNR clinical data and verify potential DTEMRL bias correction properties.

## 5.2. Noise Level Estimation

The underlying noise estimation procedure (Fig. 2) is stable, accurate, and does not depend on spatial correlations or the existence of a background region. It also avoids dealing with spatially correlated noise, which is common in DTI due to up-sampling and/or interpolation. With the widespread use of parallel imaging methods, this noise level estimator – while specifically developed for use in our improved tensor estimation procedure – could also have far wider utility beyond diffusion tensor imaging.

## 5.3. Conclusion

The bimodal performance of DTEMRL suggests an opportunity for a hybrid approach to tensor estimation even when SNR is unknown. Simulations indicate that DTEMRL either substantially improves tensor estimation or results in degraded reliability (Fig. 1) which is influenced by initialization. The newly presented noise level estimation method provides a robust SNR estimate that does not depend on tensor estimation, while the LLMMSE method estimates FA. Together, these estimates may enable a decision framework to transition between DTEMRL and LLMMSE based on expected performance.

DTEMRL provides a platform on which to develop ML approaches for robust DW image analysis, regularization, and spatial filtering. MR images are often corrupted by artifacts which are not well modeled by additive or Rician noise. Detection and/or removal of these artifacts could be accomplished directly with likelihood measures. Alternatively, DTEMRL could be desensitized to outliers through use of a robust likelihood function. Furthermore, prior probabilities could be associated with spatial distribution for tensor field regularization or with the tensors themselves to transform this maximum likelihood approach into a Bayesian maximum *a posteriori* approach. To facilitate clinical applications and further research, the DTEMRL research software may be optimized, as the current Matlab implementation requires 200 ms per voxel on a PC.

## References

1. Andersson, JL. Int Soc Magn Reson Med. Berlin, Germany: 2007. Maximum likelihood estimation of diffusion parameters with a rician noise model; p. 1881
2. Basser PJ, Jones DK. Diffusion-tensor MRI: theory, experimental design and data analysis - a technical review. NMR Biomed. 2002; 15(7–8):456–67. [PubMed: 12489095]

3. Bastin ME, Armitage PA, Marshall I. A theoretical study of the effect of experimental noise on the measurement of anisotropy in diffusion imaging. *Magn Reson Imaging*. 1998; 16(7):773–785. [PubMed: 9811143]
4. Basu S, Fletcher T, Whitaker R. Rician noise removal in diffusion tensor MRI. *Int Conf Med Image Comput Comput Assist Interv*. 2006; 9(Pt 1):117–25.
5. Bazin P-L, Zien J-MV. Integration of geometric elements, euclidean relations, and motion curves for parametric shape and motion estimation. *IEEE Trans Pattern Anal Mach Intell*. 2005; 27(12):1–17.
6. Chen B, Hsu EW. Noise removal in magnetic resonance diffusion tensor imaging. *Magn Reson Med*. 2005; 54(2):393–401. [PubMed: 16032670]
7. Cox, R.; Glen, D. *Int Soc Magn Reson Med*. Seattle, WA: 2006. Efficient, robust, nonlinear, and guaranteed positive definite diffusion tensor estimation; p. 349
8. Ding Z, Gore JC, Anderson AW. Reduction of noise in diffusion tensor images using anisotropic smoothing. *Magn Reson Med*. 2005; 53(2):485–90. [PubMed: 15678537]
9. Frandsen J, Hobolth A, Ostergaard L, Vestergaard-Poulsen P, Vedel Jensen EB. Bayesian regularization of diffusion tensor images. *Biostatistics*. 2007
10. Gudbjartsson H, Patz S. The Rician distribution of noisy MRI data. *Magn Reson Med*. 1995; 34(6): 910–4. [PubMed: 8598820]
11. Horsfield MA, Jones DK. Applications of diffusion-weighted and diffusion tensor MRI to white matter diseases - a review. *NMR in Biomedicine*. 2002; 15(7–8):570–577. [PubMed: 12489103]
12. Jones DK, Basser PJ. “Squashing peanuts and smashing pumpkins”: How noise distorts diffusion-weighted MR data. *Magn Reson Med*. 2004; 52(5):979–93. [PubMed: 15508154]
13. Koay CG, Basser PJ. Analytically exact correction scheme for signal extraction from noisy magnitude MR signals. *J Magn Reson*. 2006; 179(2):317–22. [PubMed: 16488635]
14. Niethammer, M.; Estepar, RS-J.; Bouix, S.; Shenton, M.; Westin, C-F. 28th IEEE EMBS. New York City, NY: 2006. On diffusion tensor estimation; p. 2622-2625.
15. Nowak R. Wavelet-based Rician noise removal for magnetic resonance imaging. *IEEE Trans Img Proc*. 1999; 8(10):1408–1419.
16. Pham, DL.; Bazin, P-L. Simultaneous boundary and partial volume estimation in medical images. *Int Conf Med Image Comput Comput Assist Interv*; 2004.
17. Pruessmann KP, Weiger M, Scheidegger MB, Boesiger P. Sense: sensitivity encoding for fast MRI. *Magn Reson Med*. 1999; 42(5):952–62. [PubMed: 10542355]
18. Salvador R, Pena A, Menon DK, Carpenter TA, Pickard JD, Bullmore ET. Formal characterization and extension of the linearized diffusion tensor model. *Hum Brain Mapp*. 2005; 24(2):144–55. [PubMed: 15468122]
19. Sijbers J, den Dekker AJ. Maximum likelihood estimation of signal amplitude and noise variance from MR data. *Magn Reson Med*. 2004; 51(3):586–94. [PubMed: 15004801]
20. Skare S, Hedehus M, Moseley ME, Li TQ. Condition number as a measure of noise performance of diffusion tensor data acquisition schemes with MRI. *J Magn Reson*. 2000; 147(2):340–52. [PubMed: 11097823]
21. Tschumperlé, D.; Deriche, R. DT-MRI images: Estimation, regularization and application. *Int Conf Comput Aide Sys Theory*; Las Palmas, Spain. 2003. p. 46-47.
22. Wang Z, Vermuri B, Chen Y, Mareci T. A constrained variational principle for direct estimation and smoothing of the diffusion tensor field from complex DWI. *IEEE Trans Med Imaging*. 2004; 23(8):930–939. [PubMed: 15338727]

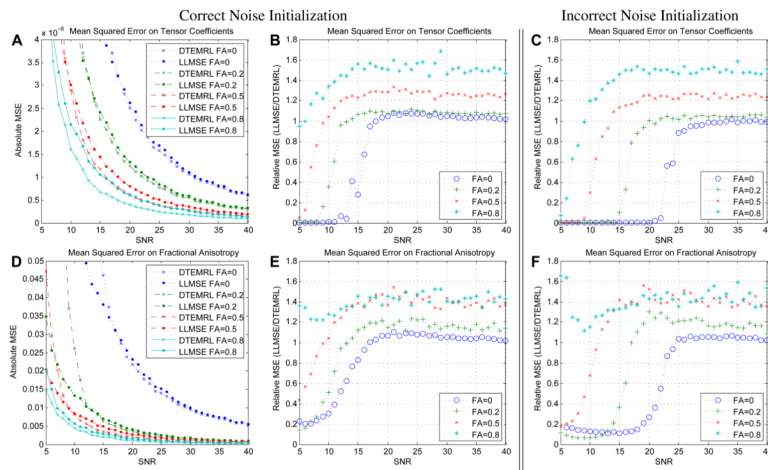


**Figure 1.** Simulation results. DTEMRL consistently improves tensor reliability in terms of tensor coefficients (A–C) and FA (D–F) when SNR is above an FA dependent threshold. Typical clinical DTI studies exhibit SNR greater than 20:1. Mis-specification of the noise level raises the threshold for improvement (B vs. C and E vs. F), but improvement magnitude is unchanged for anisotropic tensors (FA = 0.2).

\$watermark-text

\$watermark-text

\$watermark-text

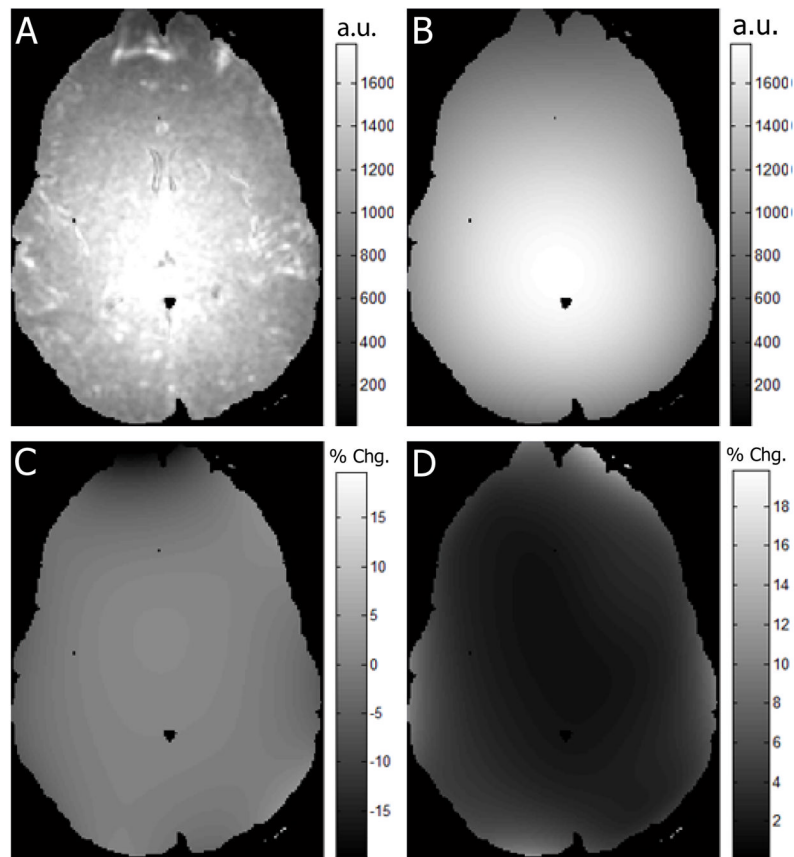


**Figure 2.** Reliability of noise level estimation. Empirical noise (A) shows clear spatial dependence. Regularization of the empirical noise (B) preserves spatial structure. The proposed noise estimation method demonstrates reliability. Both the mean difference between estimate noise and regularized empirical noise (C) and the estimated noise variability (D) are within 5 percent.

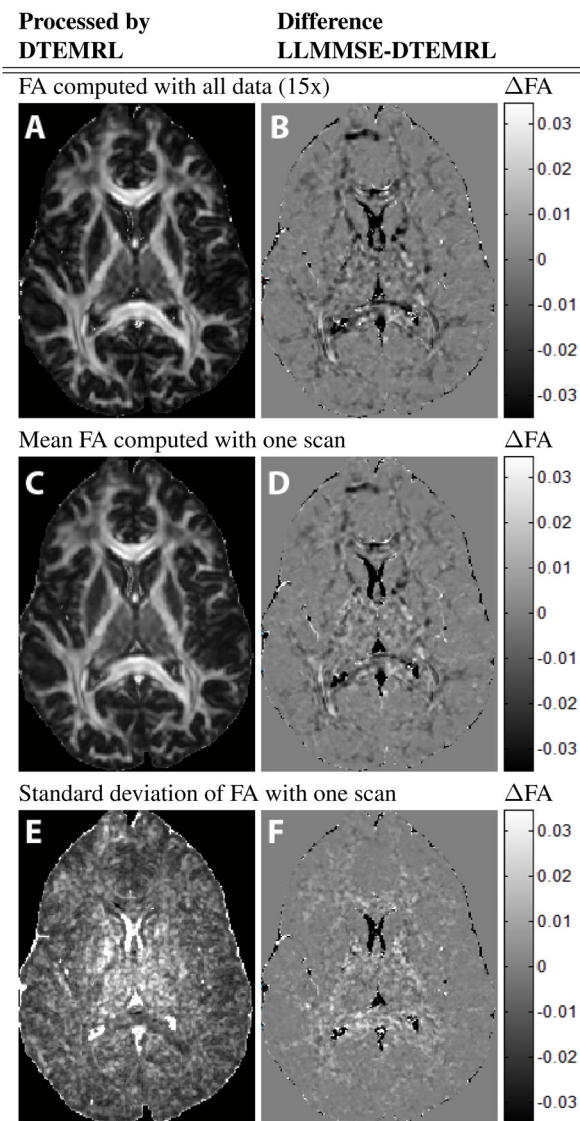


**Figure 3.** FA estimates with acquired data. Systematic bias is seen between DTEMRL and LLMSE when simultaneously using all 15 datasets (A,B). Mean differences (bias) between methods are preserved when single datasets are analyzed (C,D). Variability of DTEMRL is lower throughout the brain (E,F).

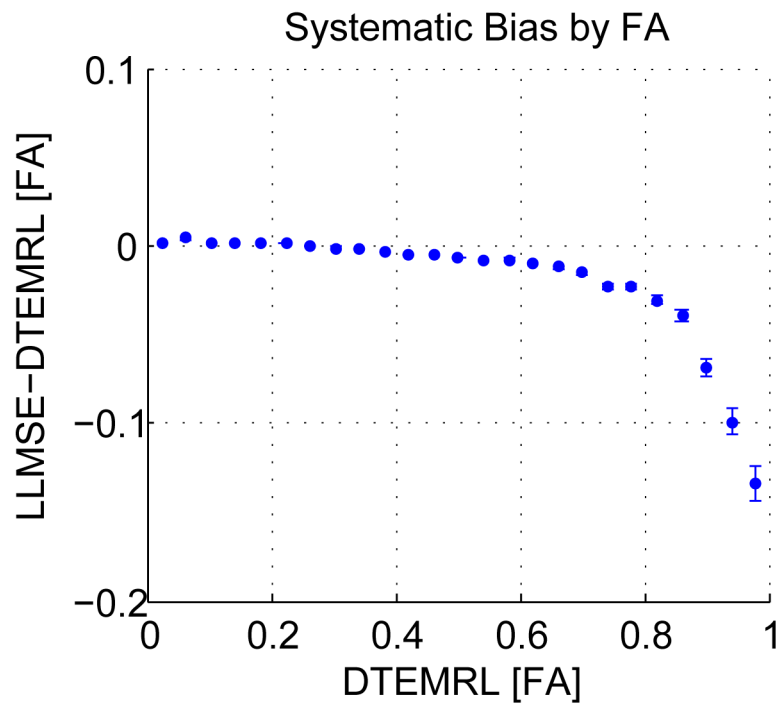


**Figure 4.** Systematic bias in FA. Mean FA binned by FA for DTEMRL and LLMSE are shown ( $\pm$ standard error).

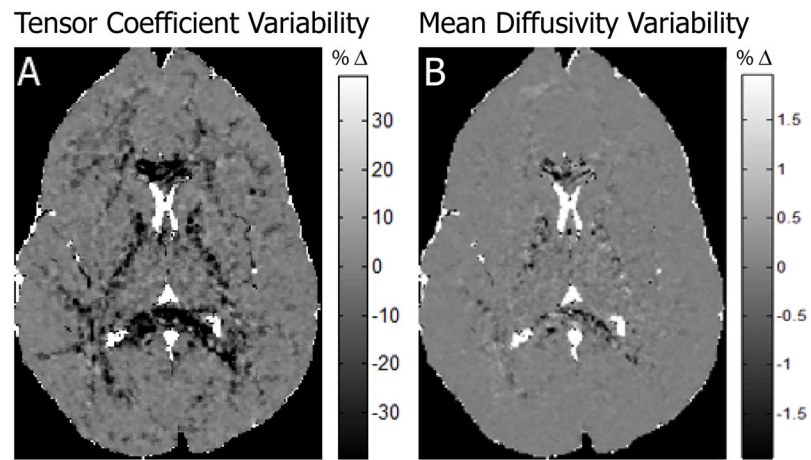
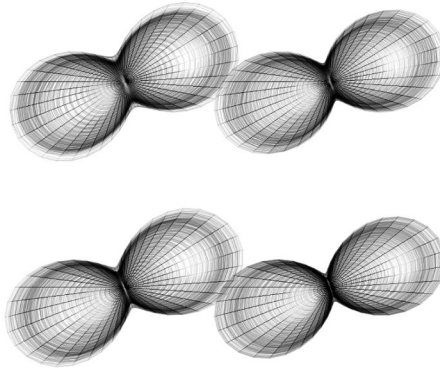


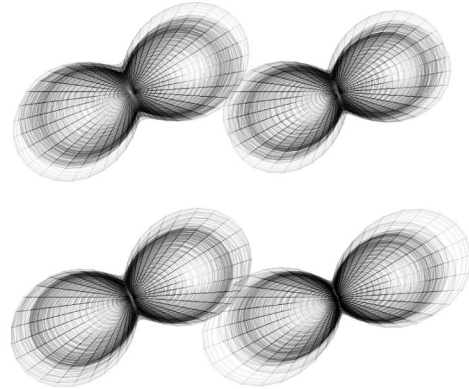
**Figure 5.** Estimation variability. Plots show the MSE of DTEMRL minus the MSE of LLMMSE for tensor coefficients (A) and MD (B). Dark tones indicate improvement with DTEMRL.

## A. Corpus Callosum

DTEMRL

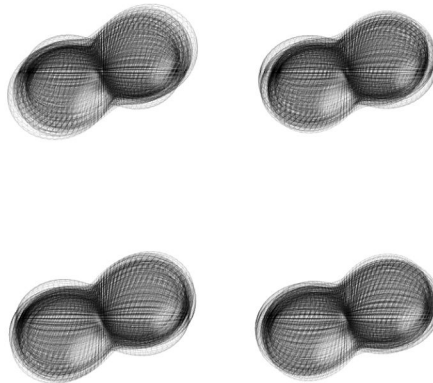


LLMMSE



## B. Internal Capsule

DTEMRL



LLMMSE

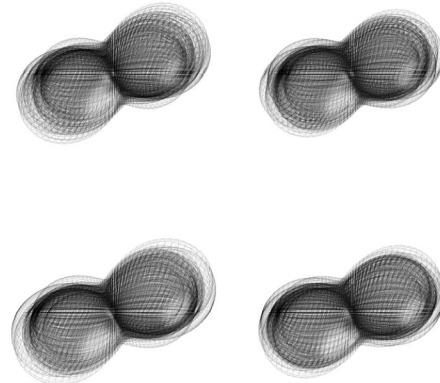


**Figure 6.** Representative tensor estimates. Renderings show all estimates for 4 voxels with DTEMRL (left) and LLMMSE (right) in the corpus callosum (A) and internal capsule (B).